

Kevlar nanofiber-functionalized multiwalled carbon nanotubes for polymer reinforcement



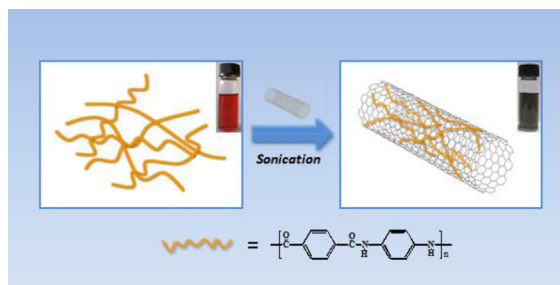
Jinchen Fan¹, Jialiang Wang¹, Zixing Shi*, Shan Yu, Jie Yin

School of Chemistry and Chemical Engineering, State Key Laboratory for Metal Matrix Composite Materials, Shanghai Jiao Tong University, Shanghai 200240, People's Republic of China

HIGHLIGHTS

- Surface functionalization of carbon nanotubes with Kevlar nanofibers.
- Functionalized carbon nanotubes can be well-dispersed in solvents.
- The nanocomposites exhibit a remarkable improvement of mechanical properties.

GRAPHICAL ABSTRACT



ARTICLE INFO

Article history:

Received 5 September 2012

Received in revised form

22 May 2013

Accepted 15 June 2013

Keywords:

Composite materials

Interfaces

Polymers

Thin films

Adhesion

ABSTRACT

Multiwalled carbon nanotubes (MWNTs) have been widely used as nanofillers for polymer reinforcement due to their excellent mechanical properties. However, for MWNTs-based polymer composites, the rigid surface, poor dispersibility and weak interaction of MWNTs still limited the potential and further application in mechanical reinforcement. In this paper, we report a facile method for functionalization of MWNTs with Kevlar nanofibers. Kevlar nanofiber-functionalized multiwalled carbon nanotubes (KNCNTs) were successfully obtained by the simple process of solution mixing followed with sonication. The as-prepared KNCNTs can be well dispersed in water and dimethylsulfoxide (DMSO) solvents. In the next, poly(vinyl alcohol) (PVA) and poly(methyl methacrylate) (PMMA) were chosen as model polymer for investigating the reinforcement effect of KNCNTs. The results of tensile tests demonstrated that the ultimate tensile strengths and Young's modulus of KNCNTs/PVA and KNCNTs/PMMA nanocomposite films were significantly improved. The KNCNTs have an advantage over the pristine MWNTs for polymer reinforcement.

© 2013 Elsevier B.V. All rights reserved.

1. Introduction

Carbon nanotubes (CNTs) have always been aroused great interests in various fields, since their outstanding thermal, electrical

and mechanical properties [1–6]. Besides, CNTs possess low density and ultrahigh aspect ratio [7,8]. Combining the outstanding properties, CNTs exhibit great potential in the application of polymer composites, especially as nanofillers for polymer reinforcement [9–11]. However, the challenges still remain and greatly restrict the full realization of excellent mechanical properties of CNTs (ultrahigh Young's modulus and tensile strength). Due to the intrinsic entangling and bundling, CNTs themselves cannot be well dispersed in common solvents and polymer matrix for CNTs-based

* Corresponding author. Tel.: +86 21 54743268; fax: +86 21 54747445.

E-mail address: zxshi@sjtu.edu.cn (Z. Shi).

¹ These authors contributed equally to this work.

polymer composites. Additionally, the rigid surfaces, associated with the smooth surface of CNTs, remarkably reduced the interfacial interaction with polymer matrix [12].

Recently, tremendous efforts have been taken on the surface modification of CNTs, primarily in order to achieve stable dispersion and good miscibility with the surrounding matrix, as well as enhance the interfacial interactions. Among various methods, physicochemical modification is more effective and has been widely adopted in the fabrication of CNTs-based polymer composites [13–15]. By introducing covalent-modifying groups on the surface of CNTs, the dispersibility was greatly improved and the functionalized CNTs exhibit excellent mechanical reinforcement effect for polymer composites. Zhu et al. found that the fluorinated CNTs can be well integrated in the epoxy resin and the resultant composites exhibited excellent mechanical properties [16]. Yang et al. reported that the grafting of polyethylene (PE) onto the CNTs enabled them well dispersed in the PE matrix and the CNTs/PE composites showed simultaneous improvement of strength, stiffness, ductility and toughness [17]. Additionally, a general modification strategy is an acid treatment which can purify CNTs and produce carbonyl groups on the surface of CNTs, thus facilitating the incorporation of CNTs into various polymer matrix as well as further functionalization [18–21]. However, these chemical modifications are usually complicated; moreover, the achievements of well dispersion and strong interfacial interaction are always at the cost of partial structure defects of CNTs which may considerably alter or disrupt their desirable properties [12,22]. In some cases, non-covalent coating of CNTs with appropriate high-performance polymer could address this dilemma and it has been reported in previous studies [23–25].

Poly(paraphenylene terephthalamide) (PPTA), known as Kevlar, possesses high tensile strength-to-weight ratio, has intrigued interests in recent years, especially in the combination of CNTs [26]. The combination of these two excellent components is believed as a promising candidate for high-performance reinforcement nanofillers for polymer composites. O'Connor et al. first reported the physical coating of Kevlar on the surface of CNTs by heating them in the mixture of sulfuric and nitric acids, and this functionalized CNTs demonstrated remarkable improvement of mechanical properties on a variety of polymers [27,28]. However, the fabrication of this novel nanomaterial has to be conducted in the concentrated acids at high temperature, so a mild and facile method to combine Kevlar and CNTs is urgently desired.

Interestingly, Kotov's group presented a novel approach to prepare nanoscale forms of Kevlar nanofibers (KNFs) with high aspect ratio by controlled deprotonation of Kevlar threads in DMSO in presence of potassium hydroxide (KOH) [29]. The resultant Kevlar nanofiber (KNF)/DMSO dispersion is very stable. Inspired, we report a facile method for functionalization of MWNTs with KNFs. The KNFKNF-functionalized multiwalled carbon nanotubes (KNCNTs) were successfully obtained by the simple process of solution mixing followed with sonication. The as-prepared KNCNTs can be well dispersed in water and dimethylsulfoxide (DMSO) solvents. In the next, poly(vinyl alcohol) (PVA) and poly(methyl methacrylate) (PMMA) were chosen as model polymer for investigating the reinforcement effect of KNCNTs.

2. Experimental

2.1. Materials

MWNTs (purity, >95%; length, ~10 μm ; and diameter, >30 nm) were purchased from Chengdu Organic Chemistry Co. Bulk Kevlar 29 was provided by DuPont. PVA with repeat unit numbers of ~2600 (PVA AH-26; hydrolysis degree, ~98%) was purchased from

Shanghai Chemical Reagents Co. (Shanghai, China). Poly(methyl methacrylate) (PMMA) (average $M_w = 70,000$) was obtained from BASF Chemical Co., Ltd (Shanghai, China). DMSO and KOH were purchased from Sinopharm Chemical Reagent Co Ltd (SCRC) and DMSO was dehydrated with 4A molecular sieve before use.

2.2. Preparation of KNFs/DMSO dispersion

KNFs/DMSO dispersion was prepared by split the bulk Kevlar-29 thread in DMSO with the aid of KOH as previously reported by Kotov's group [29]. Typically, 0.2 g of bulk Kevlar-29 thread and 0.3 g of KOH were added into 100 mL of DMSO. After magnetically stirring at room temperature for 1 week, a dark red KNFs/DMSO dispersion was finally obtained, accompanied with completely dissolved of bulk Kevlar-29 thread.

2.3. Synthesis of Kevlar nanofiber-functionalized MWNTs (KNCNTs)

Desired amount of MWNTs was added into the as-prepared KNFs/DMSO dispersion (2 mg mL^{-1}) and sonicated for 2 h to yield a homogeneous black dispersion. Next, the resultant mixture dispersion was centrifuged at 4000 rpm for 10 min to separate the unreacted MWNTs. The supernatant was dried under in an air oven at 80 $^{\circ}\text{C}$ for 48 h. Then the obtained KNCNTs powder were further washed with DMSO and H_2O , and finally dried by vacuum drying at 80 $^{\circ}\text{C}$ for another 48 h.

2.4. Fabrication of KNCNTs/PVA and KNCNTs/PMMA composite films

KNCNTs/PVA composite films were fabricated by a simple solution-casting method. A typical procedure involved the dispersion of required amount of KNCNTs in 5 mL of H_2O , and sonication to form homogeneous dispersions. Meanwhile, 1.0 g of PVA was dissolved in 10 mL of water at 90 $^{\circ}\text{C}$ for 1 h to give a 10 wt% solution. Then, these two solutions were subjected to being mixed together, with stirring of 4 h for effective mixing and sonication of 10 min for the removal of trapped air bubbles. Finally, the homogeneous KNCNTs/PVA mixture solutions were cast onto a PTFE flat plate with a diameter of 8 cm under horizontal condition and flattened to uniform thickness using a flat blade. The KNCNTs/PVA nanocomposite films were dried at 60 $^{\circ}\text{C}$ for 24 h. For completely removing the water, the KNCNTs/PVA nanocomposite films were further dried in vacuum at 80 $^{\circ}\text{C}$ for 8 h. By varying the amount of KNCNTs, the KNCNTs/PVA nanocomposite films with different weight fractions of KNCNTs were obtained. In the meantime, the KNCNTs/PMMA nanocomposite films were prepared by the same method, except for the dispersion media (DMSO, instead of H_2O). Additionally, MWNTs/PVA and MWNTs/PMMA composite films were also prepared for comparison.

2.5. Instruments and characterization

Fourier transform infrared (FT-IR) spectra were recorded on a Perkin–Elmer Spectrum 100 FTIR spectrometer. Raman spectra were taken on Bruker Optics Senterra R200-L dispersive Raman microscope. Atomic force microscopy (AFM) images were taken by digital E-sweep Atomic Force Microscope in tapping mode. Transmission electron microscopy (TEM) images were obtained from JEOL2100F. The fracture surface images of composite films were obtained from scanning electron microscope (SEM) (JSM-7410F, JEOL Ltd, Japan). Thermogravimetric analysis (TGA) was carried out in nitrogen with a Perkin–Elmer TGA 2050 instrument at a heating rate of 20 $^{\circ}\text{C min}^{-1}$. Using an Instron 4465 instrument, the measurement of tensile tests was performed on the rectangular film samples with the width of 4 mm. The condition of tensile tests were

listed as follows: crosshead speed of 5 cm min^{-1} , a load cell of 2 kN, temperature of $25 \text{ }^\circ\text{C}$, humidity of 30%, initial gauge length of 30 mm. The degree of crystallinity of samples was measured by a differential scanning calorimeter (DSC) model 6200 (Seiko, Japan).

3. Results and discussion

3.1. Preparation of KNFs/DMSO dispersion

The bulk macroscale bulk Kevlar-29 thread can be effectively split into aramid nanofibers by deprotonation in the solution system of DMSO and KOH based on the report of Kotov's group [29]. The process of splitting the bulk Kevlar-29 macroscale fibers into nanofibers is likely to occur by abstraction of mobile hydrogen from amide groups and substantial reduction the interaction of hydrogen bonds between the polymer chains. The electrostatic repulsion between the polymer chains facilitates the formation of ANFs [29]. As shown in the in-set photograph of Fig. 1a, the resultant red KNFs/DMSO dispersion is homogeneous and can keep stable for several months. The morphologies of KNFs were characterized by AFM, TEM and SEM images. The KNFs were clearly observed from Fig. 1a–c. The obtained Kevlar nanofibers are $\sim 25 \text{ nm}$ and the lengths are about several micrometers, in consistent with the previous report of Kotov's group [29].

3.2. Synthesis of Kevlar nanofiber-functionalized MWNTs (KNCNTs)

KNCNTs were synthesized by simply mixing KNFs/DMSO dispersion and pristine MWNTs followed with sonication. As well-known that aromatic Kevlar have strong affinity with the sidewall of MWNTs via π - π interaction [27,28]. As shown in Fig. 2a, the KNCNTs can be well dispersed in water and DMSO. It is attributed to the introduction of KNFs. By deprotonation in DMSO and KOH solvent system, the KNFs exhibit high reactivity and can be acted as high-performance polymeric building blocks [30]. The introduction of KNFs greatly improved the rigid surface of MWNTs. Therefore, the interaction sites of KNFs, attached on the surface of MWNTs, facilitated the dispersion of KNCNTs in DMSO and water.

TEM images offer the direct visual information for the functionalization of MWNTs with KNFs. Fig. 2b displays a typical TEM image of pristine MWNTs, showing a very smooth and clean surface. The MWNTs' tube structure can be clearly identified with inner and outer diameters along the length. After introduction of KNFs, the smooth surfaces of MWNTs became relative rough (Fig. 2c). From the enlarged TEM image (Fig. 2c, inset), it can be obviously observed that the KNF were attached on the surface of MWNT, with the width of 20.23 nm. In the meantime, from Fig. 2d, the KNF was adsorbed on outwalls surfaces of MWNT.

FT-IR spectra were also used to characterize the introduction of KNFs in the KNCNTs. As shown in Fig. 3, the characteristic

absorption peaks related to KNFs are located at ~ 1648 and $\sim 1544 \text{ cm}^{-1}$, corresponded to the C=O stretching vibrations and C–N stretching coupled modes respectively. The peaks at 1516 and 1318 cm^{-1} are ascribed to the C=C stretching vibrations of aromatic rings and Ph–N vibrations, respectively [29]. In the FT-IR spectrum of KNCNTs, it showed the corresponding absorption peaks and this confirmed that KNFs were successfully introduced into the structures of MWNTs.

Raman spectra of MWNTs, KNFs and KNCNTs are illustrated in Fig. 4. MWNTs have the obvious D band (1325 cm^{-1}) and G band (1573 cm^{-1}) which is in consistent with previous reports [31,32]. KNFs also showed some characteristic bands of C–C ring stretching (1181 , 1275 , 1511 and 1610 cm^{-1}), C–H in plan stretching (1327 m^{-1}) and C–N stretching (1567 and 1647 cm^{-1}) [29]. But for KNCNTs, these characteristic bands of KNFs cannot be remarkably observed in KNCNTs since the overlap of D and G bands. In addition, the spectrum of KNCNTs really revealed distinct changes when compared to that of MWNTs. The result demonstrated the conjunction of MWNTs and KNFs. It is consistent with the FT-IR measurement.

TGA analysis was carried out to investigate the thermal stability and component content for KNCNTs. From Fig. 5, the maximum decomposition temperature of KNFs is around $565 \text{ }^\circ\text{C}$. Toward to KNCNTs, the maximum decomposition temperature increased to $\sim 575 \text{ }^\circ\text{C}$ due to the incorporation of MWNTs. Additionally, the ratios of constituent for KNFs and MWNTs of the KNCNTs can also be determined by TGA analysis. Judging from the weight loss of KNFs and KNCNTs, it indicates that the weight ratio of KNFs is around 50%.

3.3. Fabrication of KNCNTs/PVA and KNCNTs/PMMA composite films

Poly(vinyl alcohol) (PVA) and poly(methyl methacrylate) (PMMA) were chosen as model polymers for investigating the reinforcement effect of KNCNTs. The KNCNTs/PVA and KNCNTs/PMMA composite films were prepared by a simple solution-casting method, and pristine MWNTs-based composite films were also prepared for comparison. Here, the PVA-based composites were selected to reveal the dispersibility of the nanofillers in the polymer matrix. The photographs of composite films with different loadings of KNCNTs provide direct evidence for evaluating the quality of the composite films. As shown in Fig. 6, the KNCNTs/PVA composite films are homogeneous and uniform. Increasing with the loading amount of KNCNTs, the transparency of KNCNTs/PVA composite films gradually become dark color. At a high loading of 2 wt%, there are some evident black speckles in MWNTs/PVA composite film. In comparison, the KNCNTs/PVA composite film still kept favorable dispersibility. For better understanding the dispersed state, optical microscope images were used to characterize the dispersed state for KNCNTs and MWNTs in PVA matrix. From Fig. 7b–c, the

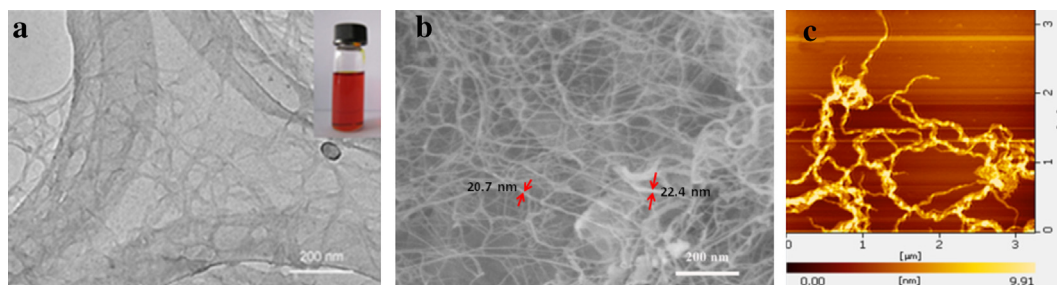


Fig. 1. (a) TEM image of Kevlar nanofibers (inset is the photograph of KNFs/DMSO dispersion with a concentration of 2 mg mL^{-1}), (b) SEM image of Kevlar nanofibers, and (c) AFM image of Kevlar nanofibers.

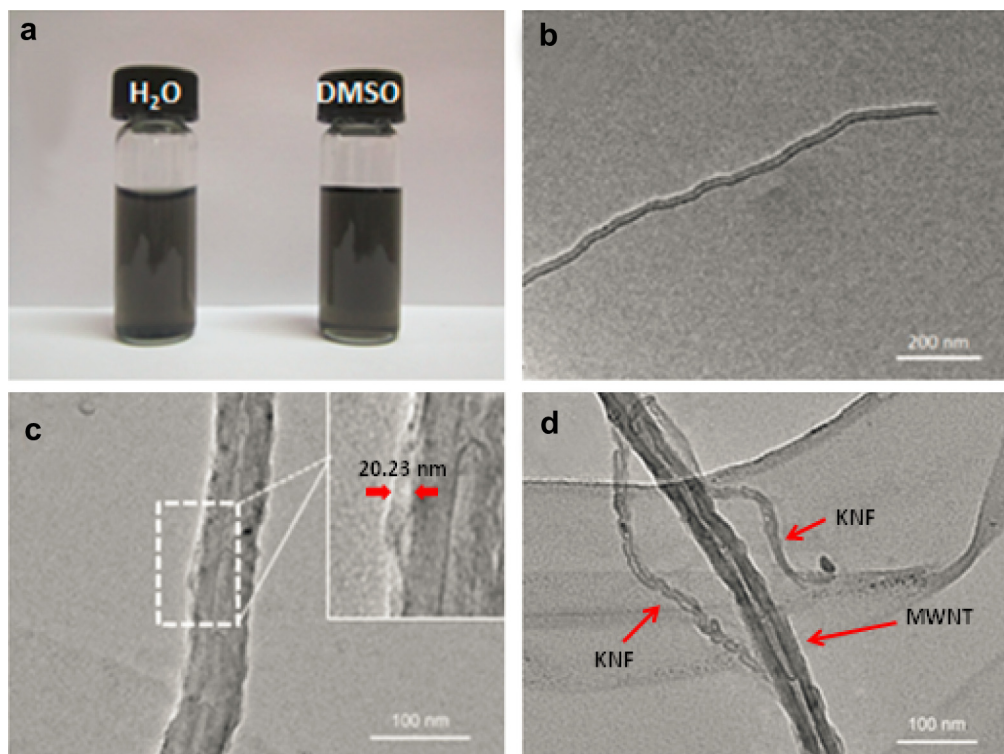


Fig. 2. (a) Photograph of KNCNTs dispersed in H₂O and DMSO with a concentration of 0.5 mg mL⁻¹, (b) TEM images of pristine MWNTs, and (c, d) KNCNTs.

KNCNTs/PVA composite films with different loading of KNCNTs were relatively homogeneous and uniform. From Fig. 7g and h, there are lots of agglomerations in the MWNTs/PVA composite films with loading of 1 and 2 wt% of MWNTs. As seen in Fig. 7e and f, the dispersed states were significantly improved with the same loading of 1 and 2 wt% of KNCNTs.

SEM images of the fracture surface of KNCNTs/PVA composite film were presented in Fig. 8. The fracture surface of PVA film was very smooth and clean. With introduction of KNCNTs, the fracture surface became relative rough for the KNCNTs/PVA composite films with 2 wt% of KNCNTs. It is clearly observed that bright dots and short lines were well distributed on the fracture surface, which were regarded as KNFs homogeneously dispersed in the PVA matrix (Fig. 8b) [31]. For the MWNTs/PVA composite film, composite films, there are obvious agglomerations and clusters across the whole fracture surfaces. Therefore, since the KNFs were used for

functionalization of MWNTs, the dispersion state of composite films was obtained obviously improvement.

Tensile test was first performed to study the reinforcement effect of KNCNTs on the mechanical properties of PVA. With the low content of pristine MWNTs, PVA/MWNTs composite films exhibit slight improvement of mechanical properties (Fig. 9a). The yield strength and Young's modulus of PVA/MWNTs composite films reach the maximum when 0.5 wt% of MWNTs was incorporated into PVA matrix, which are increase of ~32% and ~65%, respectively. However, with further increase of MWNTs loading (above 1 wt%), the maximum yield strength and Young's modulus are sharply reduced. It is attributed to the inhomogeneous dispersion of MWNTs at a high loading and the weak interaction between the MWNTs and PVA matrix which generates stress concentration and inhibits stress transfer. As previous research works, pristine MWNTs tend to exhibit some reinforcement effect at a low mass

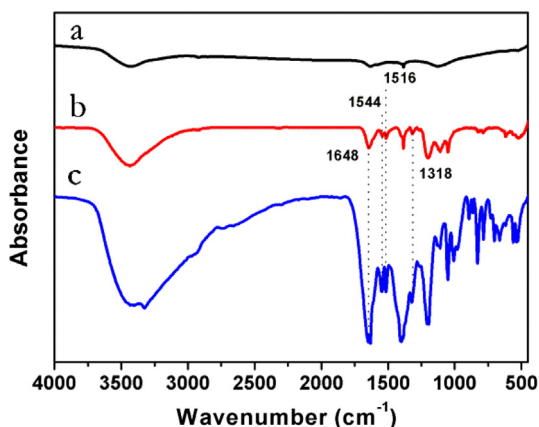


Fig. 3. FT-IR spectra of (a) pristine MWNTs, (b) KNFs, and (c) KNCNTs.

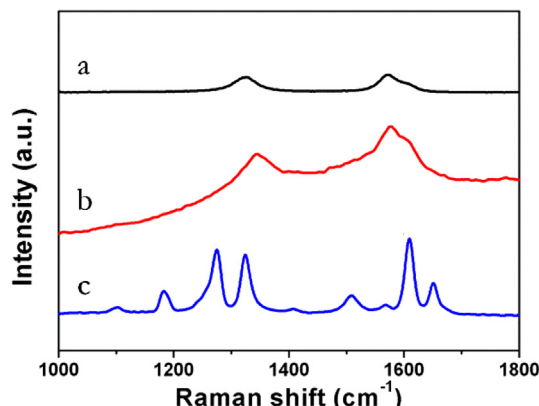


Fig. 4. Raman spectra of (a) pristine MWNTs, (b) KNCNTs, and (c) KNFs.

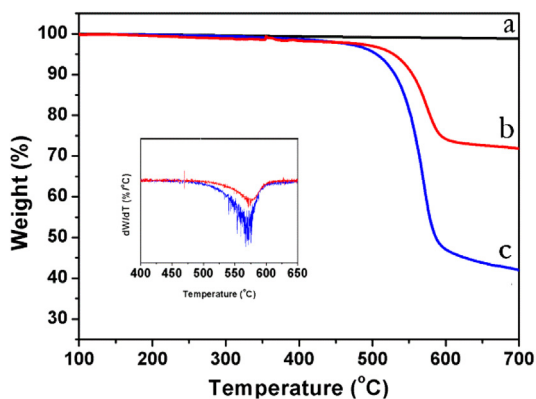


Fig. 5. TGA curves of (a) pristine MWNTs, (b) KNCNTs, and (c) KNFs.

percentage, while noticeably impair all the mechanical properties when further increasing the additive amount [32,33]. In addition, it is found that the elongation at break decreases at different extents and this may be due to the raise in brittleness. Similar phenomenon has been observed in previous studies on CNT-based polymer composites [3,6].

After functionalization of MWNTs, the KNCNTs can be acted as high-performance nanofillers for polymer reinforcement. From Fig. 9b, the yield strength and Young's modulus are almost increase in line toward to the loading of KNCNTs, and achieve maximum of ~ 122 MPa and ~ 5.86 GPa at 2 wt% loading of KNCNTs, which are $\sim 62\%$ and $\sim 86\%$ higher than the yield strength and Young's modulus of pure PVA. The KNCNTs are much better than MWNTs in enhancing the mechanical properties of PVA. It is noted that the KNCNTs/PVA composite film still keep the excellent mechanical property without the decrease of yield strength. It may be ascribed to the strong hydrogen-bonding interactions between Kevlar nanofibers attached on the surface of MWNTs and PVA chains, which enable KNCNTs to be uniformly dispersed in the PVA matrix and facilitate the stress transfer.

Furthermore, the performance on mechanical reinforcement can be reflected by measuring the increasing rate of yield strength ($d\sigma/dW$) and Young's modulus (dE/dW) of PVA-based composite film. Obviously, the slope of the fitting line ($d\sigma/dW$) for the yield strength with respect to the contents of reinforcing fillers increased from 7.4 GPa of MWNTs to 10.5 GPa of KNCNTs at a relative low loading in PVA matrix (Fig. 9). It demonstrates that the reinforcement effect of KNCNTs is much higher than MWNTs. It is worth noting that the value of dE/dW decreased from 575 GPa of MWNTs to 110 GPa of KNCNTs at a relative low loading. In fact, MWNTs can also be incorporated with PVA matrix at low loading amount and arouse the improvement of mechanical property due to exist

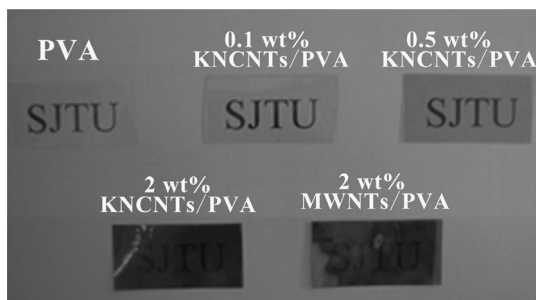


Fig. 6. Photographs of KNCNTs/PVA composite films with different contents of KNCNTs and MWNTs/PVA composite film with 2.0 wt% of MWNTs.

interactions between CNT and PVA chains [31]. But for KNCNTs, the KNFs act as both a dispersing agent and a binding agent. The KNFs solubility helps the MWNTs disperse in PVA matrix. The amido groups of KNFs can react with hydroxyl groups of PVA, which improves stress transfer between MWNTs and PVA matrix. After the introduction of KNFs into the elastic PVA film, the attached KNFs on the MWNTs primarily resist to stress and deformation and begin to slippage and break away from the surface of MWNTs. It may be resulted in the relative low value dE/dW for KNCNTs-reinforced elastic PVA film. Still, the Young's modulus of KNCNTs/PVA composite films was higher than the MWNTs/PVA films at relatively high loading content.

PVA is a semi-crystalline polymer and its mechanical properties strongly depend on the degree of crystallinity [34,35]. Polymer crystallinity can be determined with differential scanning calorimetric (DSC) by quantifying the heat associated with melting (fusion) of the polymer [36]. DSC was used to quantify the PVA crystalline fraction. The degree of relative crystallinity (χ_c) was calculated as follows:

$$\chi_c = \frac{\Delta H_m}{\Delta H_0}$$

where ΔH_m is the measured melting enthalpy of the composite films and ΔH_0 is the enthalpy of fusion for 100% crystalline PVA (138.6 J g^{-1}) [37–39]. As seen in Table S1, compared with pure PVA, no distinct changes of χ_c are found in MWNTs/PVA and KNCNTs/PVA composite films. Therefore, the remarkable improvements of strength and modulus are not related to the changes of crystallinity [40].

For further understanding the reinforcement effect of KNCNTs, PMMA were also used as model polymer. Tensile test was also conducted on MWNTs/PMMA and KNCNTs/PMMA composites. As shown in Fig. 10a, the ultimate tensile strength of MWNTs/PMMA composite film also gradually increased with the addition of pristine MWNTs at a low content (≤ 0.5 wt%), and comes to the maximum value of 34.5 MPa, which is $\sim 34\%$ higher than that of pure PMMA. The maximum Young's modulus for MWNTs/PMMA composite film reached ~ 1.6 GPa, which is $\sim 46\%$ of increase than PMMA film. However, when the content of MWNTs surpassed 0.5 wt%, the ultimate tensile strength of MWNTs/PMMA composite film was obviously reduced. But for KNCNTs/PMMA composite film, the mechanical properties are significantly improved. Both ultimate tensile strength and Young's modulus showed obvious enhancement across the whole range for content of KNCNTs. As seen in Fig. 10b, the ultimate tensile strength of KNCNTs/PMMA composite film increased from ~ 25.8 to ~ 38.7 MPa by adding only 0.2 wt% of KNCNTs, corresponded to a $\sim 50\%$ of increase compared with pure PMMA. The maximum tensile strength reaches ~ 54.2 MPa when the loading amount of KNCNTs arrives at 0.7 wt%, which is $\sim 109\%$ higher than that of pure PMMA and $\sim 57\%$ higher than the maximum tensile strength of MWNTs/PMMA, respectively. Additionally, the maximum Young's modulus of KNCNTs/PMMA is ~ 2.08 GPa, increases by $\sim 89\%$ and $\sim 30\%$, relative to pure PMMA and MWNTs/PMMA. When the loading amount of KNCNTs surpassed 0.7 wt%, the tensile strength and Young's modulus KNCNTs/PMMA composite film began to decrease. It may be attributed to poor dispersion of KNCNTs in PMMA matrix in high loading amount and the generation of agglomeration. But for MWNTs/PMMA composite film, the mechanical property became very poor as the content of MWNTs loading was higher the 0.5 wt%. To further compare the mechanical behaviors, the increasing rates of tensile strength and Young's modulus has been calculated as shown in Fig. 10. The increasing rate of strength rise from ~ 3.9 GPa of MWNTs/PMMA to ~ 6.5 GPa of KNCNTs/PMMA. Additionally, the

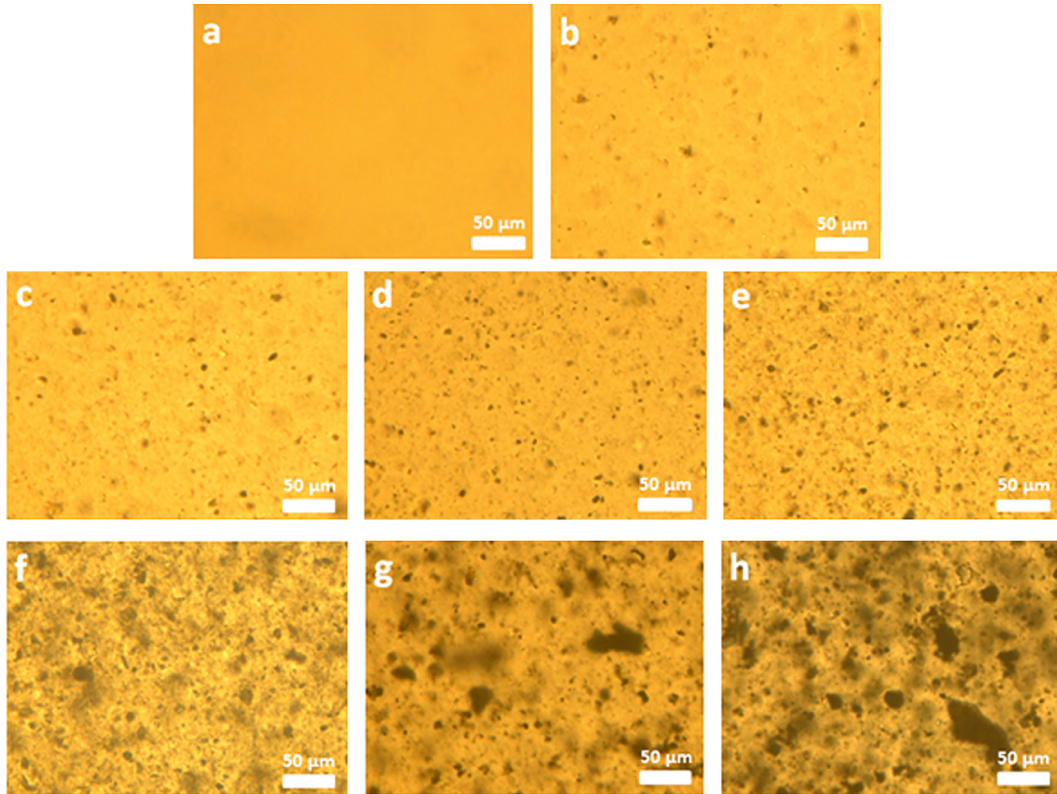


Fig. 7. Optical microscope images of (a) pure PVA, KNCNTs/PVA composite films with different contents of KNCNTs: (b) 0.1 wt%, (c) 0.2 wt%, (d) 0.5 wt%, (e) 1.0 wt%, (f) 2.0 wt%, and MWNTs/PVA composite film with different contents of MWNTs: (g) 1.0 wt%, (h) 2.0 wt%.

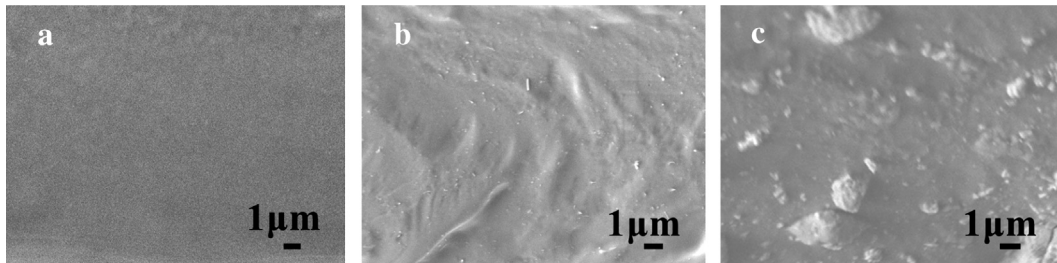


Fig. 8. SEM images of the fracture surface of (a) pure PVA, (b) KNCNTs/PVA composite film with 2 wt% of KNCNTs, and (c) MWNTs/PVA composite films with 2 wt% of MWNTs.

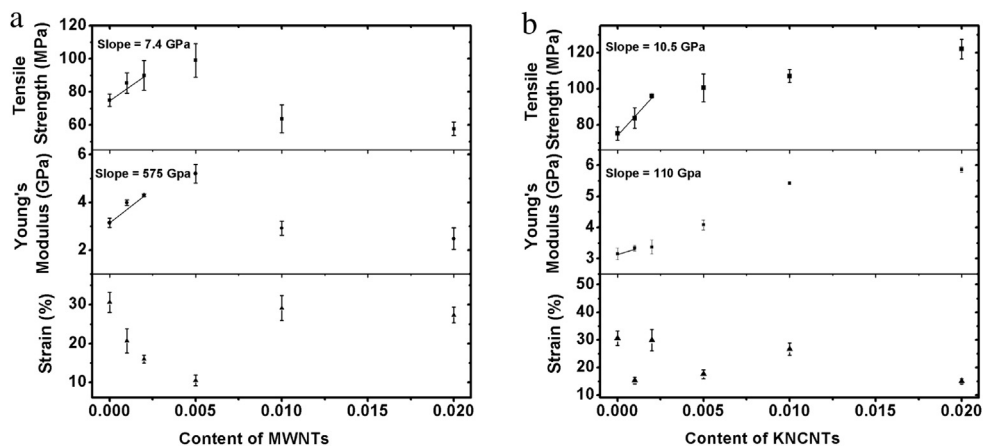


Fig. 9. Tensile strength, Young's modulus and strain for (a) MWNTs/PVA composite films with different contents of contents of MWNTs, and (b) KNCNTs/PVA composite films with different contents of contents of KNCNTs.

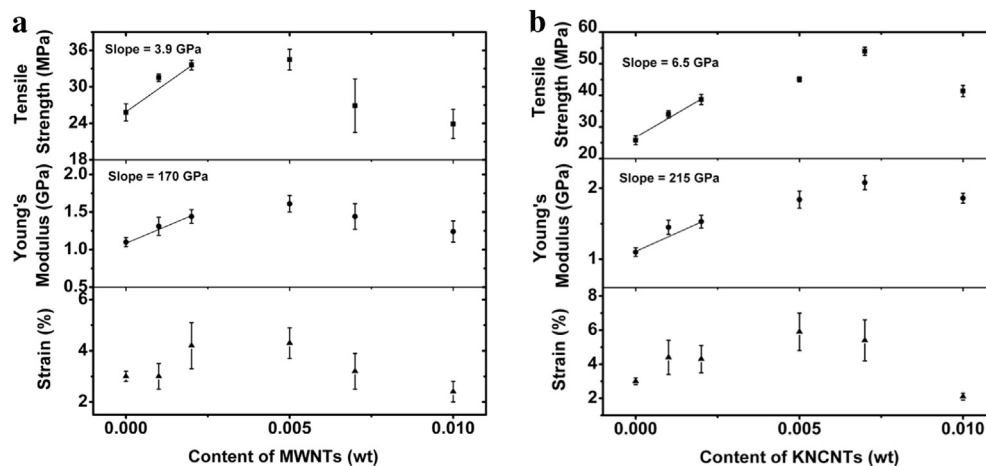


Fig. 10. Tensile strength, Young's modulus and strain for (a) MWNTs/PMMA composite films with different contents of contents of MWNTs, and (b) KNCNTs/PMMA composite films with different contents of contents of KNCNTs.

Table 1

Summary on the mechanical properties of MWNTs and KNCNTs based polymer composites.

Polymer composite	Maximum value		Increasing rate	
	Tensile strength (MPa)	Young's modulus (GPa)	Strength (GPa)	Modulus (GPa)
PVA/MWNTs	99.0	5.2	7.4	575
PVA/KNCNTs	122.0	5.9	10.5	110
PMMA/MWNTs	34.5	1.61	3.9	170
PMMA/KNCNTs	54.2	2.08	6.5	215

increasing rate for Young's modulus is the same as the tensile strength.

Obviously, the Kevlar nanofibers-functionalized MWNTs (KNCNTs) can be acted as a novel high-performance nanofillers for polymer reinforcement, e.g. PVA and PMMA. As a result, KNCNTs exhibit better dispersion effect than pristine MWNTs in polymer matrix, especially in high loading amount. In the meantime, there is strong interaction between the polymer matrix and the KNF which was attached on the surface of MWNTs. As a result, from Table 1, the maximum strength and Young's modulus for KNCNTs/PVA and KNCNTs/PMMA composite films were higher than those of MWNTs/PVA and MWNTs/PMMA composite films. Further, the increasing rates for tensile strengths of KNCNTs/PVA and KNCNTs/PMMA composite films were superior to the MWNTs/PVA and MWNTs/PMMA at a relative low loading of KNCNTs and MWNTs. In contrast, the extent for growth on the increasing rate of Young's modulus were not sharply as the tensile strength, even drop for KNCNTs/PVA composite due to the stress transfer between polymer chains and the KNFs on the surface of MWNTs. Whatever, the Young's modulus of KNCNTs/PVA and KNCNTs/PMMA still are higher than the MWNTs/PVA and MWNTs/PMMA composite films.

4. Conclusions

In summary, the KNCNTs were prepared by mixing the pristine MWNTs into the KNF/DMSO dispersion followed with sonication. The MWNTs were successfully functionalized by KNFs with π -stacking interaction. Due to the introduction of KNFs, the KNCNTs can be well dispersed in water and DMSO solvents. The KNCNTs exhibit high enhancement effect for mechanical reinforcement of PVA and PMMA-based composites. The KNCNTs exhibit better

dispersion effect than pristine MWNTs in polymer matrix, especially in high loading amount. In the meantime, there is strong interaction between the polymer matrix and the KNF which was attached on the surface of MWNTs. The results of tensile tests demonstrated that the reinforcement effect of KNCNTs was better than the pristine MWNTs. Therefore, the KNCNTs show significantly potential as novel and effective reinforcement additive in polymer composites.

Acknowledgments

The authors would like to thank the National Nature Science Foundation of China (no. 50973062) for the support. Additionally, the authors also acknowledge the staff of Instrumental Analysis Center of Shanghai Jiao Tong University for the measurement.

Appendix A. Supplementary data

Supplementary data related to this article can be found at <http://dx.doi.org/10.1016/j.matchemphys.2013.06.015>.

References

- [1] M.T. Byrne, Y.K. Gun'ko, *Adv. Mater.* 22 (2010) 1672–1688.
- [2] B.S. Shim, J. Zhu, E. Jan, K. Critchley, S. Ho, P. Podsiadlo, K. Sun, N.A. Kotov, *ACS Nano* 3 (2009) 1711–1722.
- [3] J.N. Coleman, U. Khan, Y.K. Gun'ko, *Adv. Mater.* 18 (2006) 689–706.
- [4] M. Moniruzzaman, K.I. Winey, *Macromolecules* 39 (2006) 5194–5205.
- [5] A.A. Mamedov, N.A. Kotov, M. Prato, D.M. Guldi, J.P. Wicksted, A. Hirsch, *Nat. Mater.* 1 (2002) 190–194.
- [6] J.N. Coleman, U. Khan, W.J. Blau, Y.K. Gun'ko, *Carbon* 44 (2006) 1624–1652.
- [7] D. Tasis, N. Tagmatarchis, A. Bianco, M. Prato, *Chem. Rev.* 106 (2006) 1105–1136.
- [8] J. Xiong, Z. Zheng, X. Qin, M. Li, H. Li, X. Wang, *Carbon* 44 (2006) 2701–2707.
- [9] M. Cadek, J.N. Coleman, K.P. Ryan, V. Nicolosi, G. Bister, A. Fonseca, J.B. Nagy, K. Szostak, F. Béguin, W.J. Blau, *Nano Lett.* 4 (2004) 353–356.
- [10] B. Liliame, *Polymer* 48 (2007) 4907–4920.
- [11] J.N. Coleman, M. Cadek, R. Blake, V. Nicolosi, K.P. Ryan, C. Belton, A. Fonseca, J.B. Nagy, Y.K. Gun'ko, W.J. Blau, *Adv. Funct. Mater.* 14 (2004) 791–798.
- [12] S.W. Kim, T. Kim, Y.S. Kim, H.S. Choi, H.J. Lim, S.J. Yang, C.R. Park, *Carbon* 50 (2012) 3–33.
- [13] K. Balasubramanian, M. Burghard, *Small* 1 (2005) 180–192.
- [14] C. Velasco-Santos, A.L. Martínez-Hernández, F.T. Fisher, R. Ruoff, V.M. Castañón, *Chem. Mater.* 15 (2003) 4470–4475.
- [15] Y. Lin, M.J. Meziani, Y.-P. Sun, J. Mater. Chem. 17 (2007) 1143–1148.
- [16] J. Zhu, J. Kim, H. Peng, J.L. Margrave, V.N. Khabashesku, E.V. Barrera, *Nano Lett.* 3 (2003) 1107–1113.
- [17] B.X. Yang, K.P. Pramoda, G.Q. Xu, S.H. Goh, *Adv. Funct. Mater.* 17 (2007) 2062–2069.

- [18] E. Bekyarova, E.T. Thostenson, A. Yu, M.E. Itkis, D. Fakhruddinov, T.-W. Chou, R.C. Haddon, *J. Phys. Chem. C* 111 (2007) 17865–17871.
- [19] S.H. Park, P.R. Bandaru, *Polymer* 51 (2010) 5071–5077.
- [20] N.G. Sahoo, H.K.F. Cheng, L. Li, S.H. Chan, Z. Judeh, J. Zhao, *Adv. Funct. Mater.* 19 (2009) 3962–3971.
- [21] H. Zeng, C. Gao, Y. Wang, P.C.P. Watts, H. Kong, X. Cui, D. Yan, *Polymer* 47 (2006) 113–122.
- [22] J. Chen, R. Ramasubramaniam, C. Xue, H. Liu, *Adv. Funct. Mater.* 16 (2006) 114–119.
- [23] G. Viswanathan, N. Chakrapani, H. Yang, B. Wei, H. Chung, K. Cho, C.Y. Ryu, P.M. Ajayan, *J. Am. Chem. Soc.* 125 (2003) 9258–9259.
- [24] R. Blake, Y.K. Gun'ko, J. Coleman, M. Cadek, A. Fonseca, J.B. Nagy, W.J. Blau, *J. Am. Chem. Soc.* 126 (2004) 10226–10227.
- [25] M.J. O'Connell, P. Boul, L.M. Ericson, C. Huffman, Y. Wang, E. Haroz, C. Kuper, J. Tour, K.D. Ausman, R.E. Smalley, *Chem. Phys. Lett.* 342 (2001) 265–271.
- [26] D. Tanner, J.A. Fitzgerald, B.R. Phillips, *Angew. Chem. Int. Ed.* 28 (1989) 649–654.
- [27] I. O'Connor, H. Hayden, S. O'Connor, J.N. Coleman, Y.K. Gun'ko, *J. Phys. Chem. C* 113 (2009) 20184–20192.
- [28] I. O'Connor, H. Hayden, S. O'Connor, J.N. Coleman, Y.K. Gun'ko, *J. Mater. Chem.* 18 (2008) 5585–5588.
- [29] M. Yang, K. Cao, L. Sui, Y. Qi, J. Zhu, A. Waas, E.M. Arruda, J. Kieffer, M.D. Thouless, N.A. Kotov, *ACS Nano* 5 (2011) 6945–6954.
- [30] K. Cao, C.P. Siepermann, M. Yang, A.M. Waas, N.A. Kotov, M.D. Thouless, E.M. Arruda, *Adv. Funct. Mater.* 23 (2013) 2072–2080.
- [31] Y. Wang, Z. Shi, J. Yin, *J. Phys. Chem. C* 114 (2010) 19621–19628.
- [32] J. Fan, Z. Shi, Y. Ge, Y. Wang, J. Wang, J. Yin, *Polymer* 53 (2012) 657–664.
- [33] A.A. Koval'chuk, V.G. Shevchenko, A.N. Shchegolikhin, P.M. Nedorezova, A.N. Klyamkina, A.M. Aladyshev, *Macromolecules* 41 (2008) 7536–7542.
- [34] A. Koski, K. Yim, S. Shivkumar, *Mater. Lett.* 58 (2004) 493–497.
- [35] M. Cadek, J.N. Coleman, V. Barron, K. Hedicke, W.J. Blau, *Appl. Phys. Lett.* 81 (2002) 5123–5125.
- [36] Y. Kong, J.N. Hay, *Eur. Polym. J.* 39 (2003) 1721–1727.
- [37] N.A. Peppas, E.W. Merrill, *J. Appl. Polym. Sci.* 20 (1976) 1457–1465.
- [38] S. Bhattacharyya, J.P. Salvetat, M.L. Saboungi, *Appl. Phys. Lett.* 88 (2006).
- [39] A.S. Asran, S. Henning, G.H. Michler, *Polymer* 51 (2010) 868–876.
- [40] S. Bhattacharyya, J.-P. Salvetat, M.-L. Saboungi, *Appl. Phys. Lett.* 88 (2006), 233119–233119-3.